A NUMERICAL PARAMETERIZATION OF WIND MIXING IN A TIME DEPENDENT BAROCLINIC OCEANIC GENERAL CIRCULATION MODEL

Robert William Davies

NAVAL POSTGRADUATE SCHOOL
Monterey, California

THESIS

A NUMERICAL PARAMETERIZATION OF
WIND MIXING IN A TIME DEPENDENT BAROCLINIC
OCEANIC GENERAL CIRCULATION MODEL

by

Robert William Davies

March 1975

Thesis Advisor: Robert L. Haney

SECURITY CLASSIFICATION OF THIS PAGE (When Data Entered)

REPORT DOCUMENTATION PAGE		READ INSTRUCTIONS BEFORE COMPLETING FORM
1. REPORT NUMBER	2. GOVT ACCESSION NO.	3. RECIPIENT'S CATALOG NUMBER
4. TITLE (and Subtitle) A Numerical Parameterization of Wind Mixing in a Time Dependent Baroclinic Oceanic General Circulation Model		5. TYPE OF REPORT & PERIOD COVERED Master's Thesis March 1975 6. PERFORMING ORG. REPORT NUMBER
7. AUTHOR(s) Robert William Davies		8. CONTRACT OR GRANT NUMBER(s)
9. PERFORMING ORGANIZATION NAME AND ADDRESS Naval Postgraduate School Monterey, California 93940		10. PROGRAM ELEMENT, PROJECT, TASK AREA & WORK UNIT NUMBERS
11. CONTROLLING OFFICE NAME AND ADDRESS Naval Postgraduate School Monterey, California 93940		12. REPORT DATE March 1975 13. NUMBER OF PAGES
14. MONITORING AGENCY NAME & ADDRESS(if different from Controlling Office)		15. SECURITY CLASS. (of this report) Unclassified 15a. DECLASSIFICATION/DOWNGRADING SCHEDULE

16. DISTRIBUTION STATEMENT (of this Report)

Approved for public release; distribution unlimited.

17. DISTRIBUTION STATEMENT (of the abstract entered in Block 20, if different from Report)

18. SUPPLEMENTARY NOTES

19. KEY WORDS (Continue on reverse side if necessary and identify by block number)

Wind mixing parameterization
Ocean circulation model
Seasonal temperature structure

20. ABSTRACT (Continue on reverse side if necessary and identify by block number)

This work is directed toward improving an existing general circulation model (Haney, 1974) through the inclusion of time dependent surface boundary conditions and a wind mixing parameterization.

Climatological atmospheric values, functions of time, provided the model the needed parameters in order to calculate solar insolation, longwave back radiation from the ocean,

DD FORM 1 JAN 73 1473 EDITION OF 1 NOV 65 IS OBSOLETE
S/N 0102-014-6601 |
(Page 1)

SECURITY CLASSIFICATION OF THIS PAGE (When Data Entered)

sensible heat exchange and latent heat exchange. The mixing parameterization involved the use of the Monin-Obukov length scale as a measure of the mixed-layer depth. The first law of thermodynamics was used to calculate the form of eddy flux above the mixed layer depth.

A one-dimensional model using two different types of boundary conditions was used to test various parameters and ideas. The boundary condition similar to that used in the baroclinic model produced results though an interacting system that appeared similar to observations at Ocean Station "N."

The three-dimensional model was integrated through 10 years of time. Results showed a lack of a permanent thermocline due to a strong vertical diffusion. A lack of behavior attributable to mixing was noticed, indicating the climatological winds were too weak for mixing.

A Numerical Parameterization of Wind Mixing in a Time Dependent Baroclinic Oceanic General Circulation Model

by

Robert William Davies
Lieutenant, United States Navy
B.A., San Jose State University, 1968

Submitted in partial fulfillment of the requirements for the degree of

MASTER OF SCIENCE IN METEOROLOGY

from the

NAVAL POSTGRADUATE SCHOOL
March 1975

ABSTRACT

This work is directed toward improving an existing general circulation model (Haney 1974) through the inclusion of time dependent surface boundary conditions and a wind mixing parameterization.

Climatological atmospheric values, functions of time, provided the model the needed parameters in order to calculate solar insolation, longwave back radiation from the ocean, sensible heat exchange and latent heat exchange. The mixing parameterization involved the use of the Monin-Obukov length scale as a measure of the mixed-layer depth. The first law of thermodynamics was used to calculate the form of eddy flux above the mixed layer depth.

A one-dimensional model using two different types of boundary conditions was used to test various parameters and ideas. The boundary condition similar to that used in the baroclinic model produced results through an interacting system that appeared similar to observation at Ocean Station "N."

The three-dimensional model was integrated through 10 years of time. Results showed a lack of a paramanent thermocline due to a strong vertical diffusion. A lack of behavior attributable to mixing was noticed, indicating the climatological winds were too weak for mixing.

TABLE OF CONTENTS

I. INTRODUCTION---------- 6

II. THE NUMERICAL MODEL---------- 11

A. RESOLUTION AND COMPUTATIONAL EFFICIENCY- 11

B. TIME DEPENDENT BOUNDARY CONDITIONS------ 15

C. THE MIXING PARAMETERIZATION---------- 19

III. RESULTS---------- 25

A. TYPE I BOUNDARY CONDITIONS---------- 25

B. TYPE II BOUNDARY CONDITIONS---------- 31

IV. THREE-DIMENSIONAL BAROCLINIC MODEL RESULTS-- 37

V. CONCLUSIONS---------- 41

LIST OF REFERENCES---------- 53

INITIAL DISTRIBUTION LIST---------- 55

I. INTRODUCTION

The possibilities and ramifications of accurate, long-range weather forecasts are extremely important to the United States and the world. There have been annual changes in global atmospheric weather patterns documented for some time reflected by changes in temperature, rainfall and wind patterns. Similarly, the ocean experiences variations in circulation and temperature patterns that influence fluxes across the air-sea interface and thus affect the atmospheric weather patterns.

Temperature variations appear on vertical and horizontal scales of hundreds of meters in depth, millions of square kilometers in area, and contain temperature variances of $1^{o}C$ to $2^{o}C$ above or below normal. As the fluxes across the air-sea interface of such an area represent enormous amounts of thermal energy, the presence or absence of such temperature anomalies may well influence the heat and water exchange on a scale sufficient to modify existing weather patterns. It is not certain whether the thermally anomalous patches can initiate shifts in climate or if they are a passive response to the atmosphere.

In the North Pacific Experiment (NORPAX), scientists are attempting to learn about these patches. The Main goals of NORPAX are to learn how the patches are formed and what their role might be in the exchange of heat and vapor to the

atmosphere. In the long run, scientists hope to be able to monitor ocean temperature variations by remote sensing and then to use that data to predict some features of weather patterns and climatic shifts months and years in advance.

Although reliable long range prediction is still many years away, J. Namias of Scripps Institute of Oceanography and other NORPAX scientists have discovered some interesting correlations. In many years when very intense sea surface temperature anomalies were present in the North Pacific, there were also distinct weather patterns present over the United States (Namias, 1969). Although the results are not completely conclusive, they are suggestive of a link between the Pacific temperature anomalies and the climate downwind over the United States.

The NORPAX work is concentrated in several areas, however, only the theoretical/numerical area is pertinent to this thesis. Numerical models attempt to simulate the ocean dynamics and numerically integrate in time to form predictions. Since NORPAX deals with temperature anomalies on the order of $1^{o}C$ - $2^{o}C$, accuracy in the description of upper ocean dynamics is essential. Thus all advection, diffusion, convection, and wind mixing should be as accurately portrayed as possible.

The numerical model on which this work was based is that of Haney (1974). This was a 6-level model of a baroclinic ocean with flat bottom and rectangular coastline from $51.25^{o}S$ latitude to $48.75^{o}N$ latitude. The primary goal of this work was to make improvements in his model so it could be used to

predict the formation and evolution of the large-scale, sea-surface temperature anomalies described above. The improvements made were of two general types: improvements in resolution and improvements in parameterizing the physical processes.

In order to improve accuracy in the model, especially in the upper layers, Haney's model was expanded to 10 layers. The layers were made thinner in the upper ocean for resolution considerations. In addition, the geographical domain was reduced to include that part of the North Pacific Ocean bounded by the equator and 65^{o}N. Of course decreasing grid sizes alone could not suffice to enhance accuracy. The dynamics of the model had to be modified to provide appropriate parameterizations of the pertinent physical processes. Improvements were therefore made in calculating the surface fluxes and in parameterizing the effects of wind mixing.

Haney's 1974 model used a simple linearized equation to calculate the heat fluxes across the air-sea interface;

$$FLUX = K\ (T_a - T_{sfc}) \qquad (1)$$

where T_a was an equilibrium air temperature and T_{sfc} was the predicted sea-surface temperature. K was a coefficient estimating the combined effects of sensible heat flux, upward long-wave radiation, latent heat release and downward short-wave solar radiation. In the improved version of Haney's model, each of the above surface fluxes was individually computed using prescribed atmospheric data. The atmospheric

data included incoming solar radiation, cloud coverage, surface air temperature, vapor pressure, and both north-south and east-west components of the surface geostrophic wind. In the actual time integration of the model the fluxes were at first computed using annual mean atmospheric parameters. After initial shocks in the model decreased, the first two annual harmonics of the atmospheric parameters were introduced to give time-dependent boundary conditions.

Haney's model provided vertical sub-grid scale heat fluxes through diffusion and convective adjustment. Vertical eddy diffusion of heat was accomplished with a constant diffusion coefficient whose magnitude was appropriate for the deep ocean. This process was retained along with the convective adjustment, but a new wind-mixing parameterization was introduced. According to recent mixed layer theories, (Denman, 1973), above a certain mixed-layer depth, wind generated turbulence and surface convections should both serve to mix heat downward across the interface. With finer vertical resolution in the improved model, vertical eddy diffusion using a constant coefficient was not adequate.

The surface stress used in Haney's (1974) model was an idealized one based on the mean zonal wind stress for all oceans combined (Hellerman, 1968). In the improved model, data from the North Pacific Ocean was used. As with the improved heat flux scheme, annual mean stresses were used at first until the initial shocks decreased. Then the first

two annual harmonics of the winds were added to give time dependency. Thus, the stress supporting both the circulation and the mixing were made time dependent.

II. THE NUMERICAL MODEL

A. RESOLUTION AND COMPUTATIONAL EFFICIENCY

As stated above, the basic model used in this work was that of Haney (1974). Many improvements were made in the model to effect the desired modifications. "The model is based on the hydrostatic and Boussinesq approximations. This means that the ocean is assumed incompressible, and the density is replaced by a constant everywhere except in the hydrostatic equation where it is multiplied by the acceleration of gravity. A major simplification is the neglect of salinity and the assumption that the density is a linear function of temperature alone."[1]

The reader is referred to Haney's 1974 publication for details but in the interest of completeness the following basic equations are reproduced. The equations of motion;

$$\frac{du}{dt} = \frac{-1}{\rho_o a \cos\phi}\frac{\partial p}{\partial \lambda} + fv + \frac{u}{a\cos\phi}v\sin\phi + A_m \nabla^2 u + k\frac{\partial^2 u}{\partial z^2} \quad (2)$$

and

$$\frac{dv}{dt} = \frac{-1}{\rho_o a}\frac{\partial p}{\partial \phi} - fu - \frac{u}{a\cos\phi}u\sin\phi + A_m \nabla^2 v + k\frac{\partial^2 v}{\partial z^2}\ , \quad (3)$$

---

[1] Haney, Robert L., "A Numerical Study of the Response of an Idealized Ocean to Large-Scale Heat and Momentum Flux," Journal of Physical Oceanography, v. 4, No. 2, p. 147, 1974.

The hydrostatic equation;

$$\frac{\partial p}{\partial z} = -\rho g \tag{4}$$

The mass continuity equation;

$$\frac{\partial w}{\partial z} + \frac{1}{a \cos\phi}\left[\frac{\partial u}{\partial \lambda} + \frac{\partial}{\partial \phi}(v \cos\phi)\right] = 0. \tag{5}$$

The first law of thermodynamics;

$$\frac{dT}{dt} = A_H \nabla^2 T + k \frac{\partial^2 T}{\partial z^2} + \delta_c(T) \tag{6}$$

The equation of state;

$$\rho = \rho_o \left[1 - \alpha(T - T_o)\right] \quad . \tag{7}$$

The symbols are listed in Table (1) for clarity.

TABLE 1

SYMBOL	DEFINITION
t	time
λ	longitude
ϕ	latitude
z	depth
Ω	angular speed of the earth's rotation
f	Coriolis parameter (= 2 sinΩ)
a	radius of the earth
g	acceleration of gravity
u	eastward velocity component
v	northward velocity component
w	vertical velocity component
T	temperature
T_o	constant reference temperature
ρ	density
ρ_o	density of water at reference temperature
α	coefficient of thermal expansion,

Several improvements were introduce to improve the resolution of the model. Since the work was expressly designed to improve accuracy in the sea-surface temperature, the vertical resolution had to be adjusted. The model was vertically expanded to ten levels fixed at 10, 30, 60, 100, 150, 225, 350, 700, 1500, and 3000 meters. These locations provided greater precision in the top-most layers of the ocean. This was in consonance with the effort to better parameterize the effects of wind and vertical motions which are so important in changing the temperature in the upper layers of the ocean. The total depth of the ocean remained constant at 4000 meters.

The horizontal gridding was also altered. In the original model, the latitude-longitude grid intervals were 2.5^{o} and 3.0^{0} respectively. In the present model, the latitude-longitude grid intervals were 2.0^{0} and 2.8^{o} respectively. Since the actual location of the domain was altered, the lateral boundary conditions were altered at the southern boundary (equator) where a free slip (no friction) condition was imposed.

Many schemes for improving the computational efficiency of the model were attempted; those having favorable trade-offs between computer space and computer time were retained. By far the most successful ploy involved a very fast Poisson equation solver designed by Roland Sweet (1972). The model used a streamfunction Ψ to predict the vertically averaged mean currents $(\bar{u}, \bar{v})$. The streamfunction tendency was

previously obtained by solving the Poisson-type equation every time step by over-relaxation techniques. Even though an optimum over-relaxation factor had been used, the use of the direct solver produced a savings in computer time of approximately 30%. This figure, however, is variable depending on the portion of the program dealing with the solution of the Poisson equation. If a model spends a large percentage of its time in solving the Poisson equation, a much greater percent of savings can be realized. A barotropic model or a baroclinic model having fewer vertical levels would be such an example.

An attempt at eliminating repeated multiplications every time step was made. Because of the spherical grid, all transports of heat and momentum had to be weighted by their appropriate area or volume. The various combinations of grid sizes (e.g. $\Delta x \times \Delta y$) were stored and called from core when used vice their repeated multiplication. It was found that this ploy made insignificant savings in time while expanding computer space greatly. It was thought the time spent dealing with the indices associated with the storage was comparable to the multiplications. This may not be the case on a different computer. All work discussed herein was performed on the IBM 360.

Another attempt at economizing time was to eliminate the need to switch the fields associated with one time (say t_1) and the previous time ($t_1 - \Delta t$) before calculating the friction terms. In the original model, this switching was

done every time step except every tenth step which employed a Matsuno scheme. This was altered so that the fields were switched only at the infrequent Matsuno steps. Again the time savings was small in that only a small portion of time was spent doing this operation. However the scheme did not create a need for storage expansion and did seem more logical in its notation and was therefore retained.

B. TIME DEPENDENT BOUNDARY CONDITIONS

In addition to improvements in resolution and efficiency, improvements were made in representing the physical processes. These changes were in two main areas, the first of which was in the calculation of the fluxes of heat and momentum at the sea surface.

As shown in Eq.(1), Haney's 1974 model employed a simple linearized version of heat flux. In an earlier paper, Haney (1971), formulated the flux by separately calculating the incoming solar radiation (Q_I), the net upward longwave radiation (Q_B), the latent heat exchange (Q_E), and sensible heat exchange (Q_H). The net downward heat flux Q was then;

$$Q = Q_I - (Q_B + Q_E + Q_H). \tag{8}$$

The present model employed this method of calculating the heat flux. Back radiation Q_B was calculated from

$$Q_B\ (T_o) = Q^*\ \sigma\ T_o^4 \tag{9}$$

where σ was the Stefan-Boltzman constant, T_o was the

sea-surface temperature calculated by the model, and

$$Q^* = .985\ (.39 - .05\ e_a^{\frac{1}{2}})\quad (\ 1 - .6C^2\ ) \tag{10}$$

where e_a was the atmospheric vapor pressure at 10 meters and C was the fraction of cloud coverage. This dependence of Q^* on vapor pressure and cloud coverage parameterized the reduction of upward longwave radiation by water vapor and clouds in the atmosphere.

The latent heat flux (Q_E) from the ocean was

$$Q_E = .622\rho_a\ C_D\ |V|\ L\ [e_s(T_o) - e_a]\ /P_a \tag{11}$$

where ρ_a was the density of the air, C_D was the drag coefficient, $|V|$ the wind speed at anenometer level, L the latent heat of vaporization and P_a the atmospheric pressure. The vapor pressures $e_s(T_o)$ and e_a were the saturation vapor pressure at the sea surface temperature and the atmospheric vapor pressure at 10 meters, respectively.

Sensible heat exchange (Q_H) across the interface was given by

$$Q_H = \rho_a\ C_D\ |V|\ C_p\ (T_o - T_a) \tag{12}$$

where C_p was the specific heat of air at constant pressure and T_a was atmospheric temperature at 10 meters.

Incoming solar radiation (Q_I) was calculated with

$$Q_I = S_o\ (.74 - .6C). \tag{13}$$

This expression parameterized the albedo of a cloudless

atmosphere due to air molecules, dust and water vapor scattering plus the albedo of clouds. S_o was the solar insolation incident on a horizontal surface at the top of the atmosphere. Parameters not discussed in Equations (8) - (13) are given in Table (1). The above heat flux components were calculated at each time step from the sea surface temperature predicted in the model and the atmospheric parameters which were specified on a time-dependent basis.

In addition to the thermal forcing, the ocean circulation was also forced by surface winds given on a time-dependent basis. Assuming an average geostrophic inflow angle of 10^{o} and a frictional reduction of velocity by 10%, one could derive the surface stress from the surface geostrophic winds. if u and v are the eastward and northward surface winds, respectively, after inflow and frictional influences are considered, then

$$|V| = (u^2 + v^2)^{\frac{1}{2}}$$

and the stresses

$$\tau_x = \rho_a C_D |V| u \qquad (14a)$$

$$\tau_y = \rho_a C_D |V| v \qquad (14b)$$

The atmospheric data representing monthly climatology was obtained through various sources. Solar insolation values were obtained from the Smithsonian Meteorological Tables (List, 1963, Table 132). Monthly values of the cloud coverage

were obtained from the satellite based cloud atlas of Miller (1971). Monthly values of the surface (10 meters) air temperature, vapor pressure and zonal and meridional geostrophic wind components were all obtained from an NCAR data tape of the Northern Hemisphere Climatological Atlases of Jenne et. al. (1974).

In order for the ocean model to simulate a realistic monthly normal climatology, the atmospheric wind and thermal forcing which drives the circulation must vary in a continuous manner over the annual period. To provide this continuity in the atmospheric forcing, the annual mean and the amplitude and phase of the first two harmonics were calculated from the above climatological data. The data was averaged along each grid latitudinal line with the exception of v, the northward component of the surface geostrophic wind, which was averaged along each meridion.

Thus, the atmospheric forcing was completely specified on a continuous time dependent basis. In operation, the atmospheric variables were employed in two stages. The first stage used only the annual mean data. Starting from conditions of rest and temperature a function of ϕ and z only, the integration was continued for about 5 years until the initial oscillation "settled" down. Initial shock was severe due mainly to large shear currents and boundary effects. The model was then subjected to the time dependency in the atmospheric boundary conditions. It was expected that temperature change, in the upper few hundred meters, due to

diffusion from the surface would occur within 10 years. Also, the initialization was thought to be a good estimate of actual conditions. Thus, since the depth of interest was the upper ocean, and the seasonal variation would be dominant there, a further integration was not carried out.

C. THE MIXING PARAMETERIZATION

The most important change in the model was a parameterization of the effects of wind generated mixing based upon the mixed layer theories of Kraus and Turner (1967) and Denman (1973). The change was two-fold in that both the depth to which mixing was to take place and the form of the mixing needed to be parameterized.

The parameterization of vertical eddy fluxes in the mixed layer involved the critical assumption that the Monin-Obukov (M-O) length scale determined the depth in the ocean to which mixing occurred. This depth is generally understood to be the depth at which mixing due to buoyancy forces (convection) is of the same magnitude as the mixing which is mechanically driven. At a depth less than the M-O length, mechanical mixing would dominate whereas at a depth greater than the M-O length, mixing would be predominately due to buoyancy forcing.

From Phillips (1966), the equation for the M-O length, with buoyancy fluxes due to salinity neglected, was

$$h = w_*^3/(\kappa\ g\ \alpha\ Q) \qquad (15)$$

where

$$w_* = \left\{ \left[\left(\frac{\tau_x}{\rho}\right)^2 + \left(\frac{\tau_y}{\rho} \right)^2 \right]^{\frac{1}{2}} \right\}^{\frac{1}{2}} \qquad (15)$$

and κ was the von Karman constant.

The net downward heat flux Q could have been extremely small in some cases. This would have led to an inordinately large value of h. In the model however, this mixed layer depth was not allowed to extend below the top of the model's bottom layer. A more realistic procedure would have been to constrain the depth to less than w_*/f where f was the Coriolis parameter. Both constraints were attempted with no ill effects (see results). In operation

$$h = \min \left(h_{mo}, \frac{w_*}{f}\right)$$

where h_{mo} was the M-O length. This gave the depth to which surface originated mixing extended.

The question then was what form the mixing would take. To determine this, the first law of thermodynamics was written:

$$\frac{\partial T}{\partial t} + \nabla\cdot(VT) + \frac{\partial}{\partial z}(wT) = A\,\nabla^2 T + \frac{\partial S}{\partial z} - \frac{\partial F}{\partial z} + \delta_c(T) \qquad (17)$$

where

$$F = -\,k\,\frac{\partial T}{\partial z} + (\overline{w'T'})$$

This was similar to Haney's (1974) equation with the addition of the $(\overline{w'T'})$ term representing the vertical mixing of heat due to eddy fluxes. Although in the model, T and V were not necessarily independent of z above h, this was

assumed for the purpose of calculating the wind mixing term. Also for this purpose the convective adjustment term $\delta_c(T)$ was assumed to be negligible. Thus, equation (17) could be written

$$\frac{\partial T}{\partial t} + \bar{\nabla}\cdot(VT) + \frac{\partial}{\partial z}(wT) - A\nabla^2 T - k\frac{\partial^2 T}{\partial z} - \delta_c(T) = \frac{\partial S}{\partial z} - \frac{\partial(\overline{w'T'})}{\partial z}$$

and by the above assumptions the left hand side was independent of z. This result is comparable to those of the one dimensional mixed layer theories in which advection, diffusion and convective adjustment are neglected altogether, and T is assumed independent of z in the mixed layer. Thus

$$\frac{\partial S}{\partial z} - \frac{\partial(\overline{w'T'})}{\partial z} = b \qquad (b = \text{constant})$$

and integrating to an arbitrary z

$$S(z) - (\overline{w'T'})_z = a + bz \quad \text{(linear in z)}.$$

Applying the boundary conditions a z=0 and z=-h, the constants a and b were determined:

for $z=0$ $\quad a = S_o - (\overline{w'T'})_o$

$z=-h$ $\quad a - bh = S_{-h} - (\overline{w'T'})_{-h}$

or

$$b = \frac{1}{h}\left[a - (S_{-h} - (\overline{w'T'})_{-h})\right] .$$

Substituting into the integrated thermodynamic equation one obtains

$$(\overline{w'T'})_z = (\overline{w'T'})_o + z/_h \left[(\overline{w'T'})_o - (\overline{w'T'})_{-h}\right] + S(z)$$

$$- \left\{ S_o + z/_h \left[S_o - S_{-h}\right] \right\} \qquad (18)$$

The expression for $(\overline{w'T'})_{-h}$ came from the vertical integral of Eq.(18) and use of the steady state turbulent kinetic energy equation

$$\int_{-h}^{o} (\overline{w'T'})_z \, dz = D - G \qquad (19)$$

where D and G are dissipation and generation of turbulent kinetic energy respectively. Integrating Eq.(18) from (-h) to 0, and using Eq.(19), the resultant equation was solved for $(\overline{w'T'})_{-h}$:

$$(\overline{w'T'})_{-h} = \overbrace{-2/_h(G - D)}^{1} - \overbrace{(\overline{w'T'})_o}^{2} +$$

$$\overbrace{S_o + S_{-h} - 2/_h \int_{-h}^{o} S(z)dz}^{3}. \qquad (20)$$

The terms on the right hand side were the contributions to thermal flux through the mixed layer at -h. Term 1 represented the contribution of wind mixing, term 2 that of convective mixing and term 3 the stabilizing effect due to absorption of solar radiation. The effects of solar heating were interpreted as follows by Han (private communication). If the ocean were completely opaque to solar radiation the result would enhance stability. If the flux of solar radiation had a linear profile with depth, there would have been no effect

on stability. This was due to a uniform heating throughout the layer (see Fig. 1). If the flux took on an exponential profile with depth, the effect would have been one enhancing thermal stability.

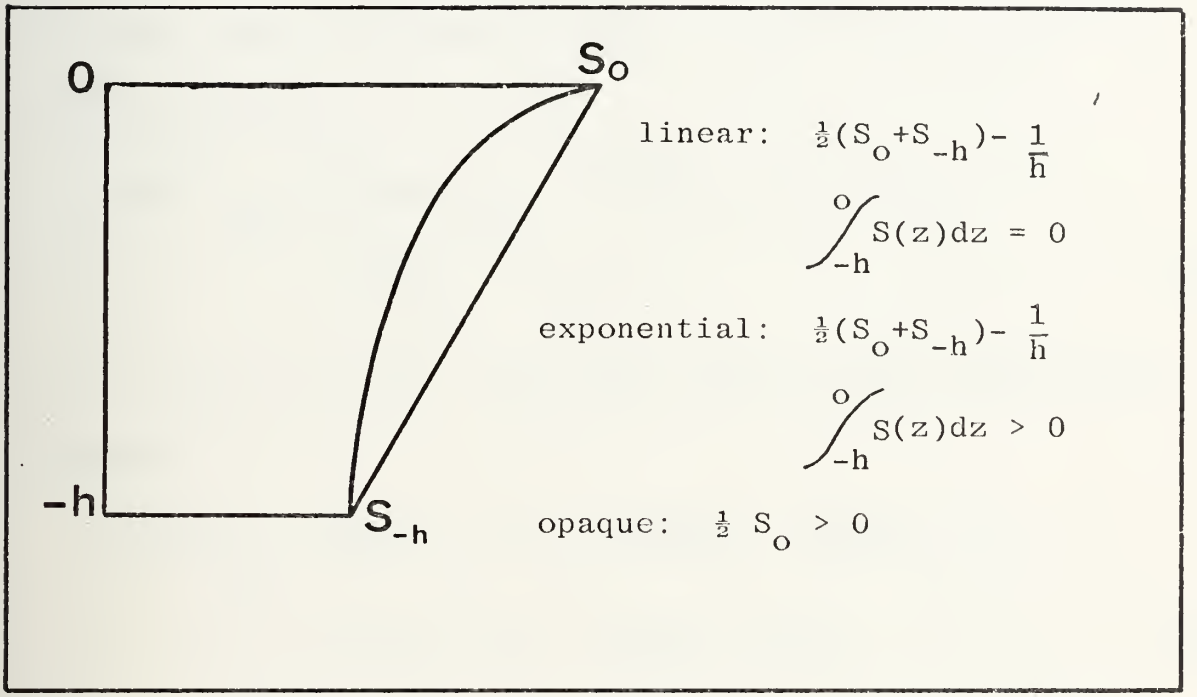

Figure 1. The stabilizing effect of solar radiation.

Paulson (1974) recently found that the profile of solar flux in the ocean could be satisfactorily represented exponentially. On a scale consistent with this model, he found

$$S(z) = S_o\, e^{(\beta' z)}$$

where $z < 0$ and $\beta' = (1/19)m^{-1}$.

The generation of turbulent kinetic energy similar to Denman (1973) took the form

$$G = \beta w_*^3 / \alpha g$$

where $\beta \sim 1.0$. The dissipation D was assumed zero.

Thus, the defining equations for $(\overline{w'T'})_{-h}$ and $(\overline{w'T'})_z$ were formulated:

$$(\overline{w'T'})_{-h} = \frac{-2}{h}\left(\beta w_*^3 / \alpha g\right) - (\overline{w'T'})_o + S_o + S_{-h}$$

$$\frac{-2}{\beta' h}(S_o - S_{-h}) \qquad (21)$$

and, thus the general expression for the heat flux may be written:

$$(\overline{w'T'})_z = (\overline{w'T'})_o + z/h\left[(\overline{w'T'})_o - (\overline{w'T'})_{-h}\right]$$

$$+ S(z) - S_o - z/h(S_o - S_{-h}) \qquad (22)$$

If the value of $(\overline{w'T'})_{-h}$ calculated from Eq. (21) was positive, indicating upward heat flux at -h, then $(\overline{w'T'})_{-h}$ was set to zero. This criteria was set upon $(\overline{w'T'})_{-h}$ because the interface below the mixed layer is essentially thermally stratified. Wind mixing would tend to reduce the stratification, never giving an upward flux of heat.

III. RESULTS

A. TYPE I BOUNDARY CONDITIONS

In order to test various aspects of the mixing parameterization before applying it to the three-dimensional, baroclinic model, a one-dimensional model was devised. In this model, horizontal variations were neglected and therefore no vertical motions due to continuity equation considerations were present. The consequence was a vertical "pole" of ocean in which temperature was affected by flux across the air-sea interface, convection, wind mixing and vertical diffusion.

The boundary conditions on the interface flux were prescribed in two ways. In TYPE I, a time-dependent heat flux was specified (Fig. 2) guaranteeing that the integral of interface flux over the annual cycle was zero. This ensured that the model would neither heat nor cool excessively. In TYPE II, a time-dependent air temperature was prescribed from which the heat flux was determined. The condition did not ensure a zero annual average but ensured that the "pole" ocean would seek an equilibrium heat content and distribution that would eventually repeat itself over the annual cycle.

Neglecting horizontal variations and motions, the first law of thermodynamics was written

$$\frac{\partial T}{\partial t} = -\frac{\partial F}{\partial z} + \delta_c(T) \qquad (23)$$

where

$$F = -k \frac{\partial T}{\partial z} + (\overline{w'T'}),$$

Thus the change in temperature was due to four physical processes: diffusion, convection, eddy flux due to wind mixing, and surface eddy flux.

Many tests were made using both types of boundary conditions. In several instances one physical process was omitted to test its significance. Other tests included modifications of constants employed and variables prescribed. After evaluation, a standard run was selected on the basis of comparisons with other runs and observations. Figures 3a and 3b represent the standard TYPE I run, and show temperature as a function of time and depth. The ocean was initially isothermal at 20^{o}C down to a depth of 4000 meters. Since the changes in temperature were surface oriented, and since there were no vertical motions, there existed no permanent thermocline. Thus the depth of interest was somewhat shallow and the graph extends to only 280 meters. As in all runs made, the graph represents the twentieth year of integration, time increasing left to right.

As seen in Fig. 3a there exists a basic asymmetry between the spring and fall periods. In spring, surface heat flux is downward tending to warm the ocean. However, only diffusion and wind mixing transport the heat down. Since h is extremely small, the heating is confined to the upper layers. In fall heat flux is upward tending to cool the

surface layers. However, in this case convection causes the entire column to be cooled forming the abrupt isothermal layers. The temperature variation lags the boundary condition heat flux input by approximately 2.0 months. The maximum heat flux occurs July 1 and the maximum sea-surface temperature occurs about August 25. Figure 3b is a series of soundings taken at the times shown. Figure 3c is a graph of the mixed layer depth h and the surface heat flux Q as functions of time. The flux is represented by a simple cosine function with a zero phase angle. The Monin-Obukov length h is calculated as in Eq. (15).

The first test performed on the TYPE I model was a comparison and significance test on the effects of diffusion. The regular diffusion coefficient k=1.5 $cm^2 sec^{-1}$ was consistent with deep ocean dynamics as explained by Munk (1966). The experiment was to see if the variation of k would change the annual temperature distribution. k was arbitrarily raised by an order of magnitude over Munk's value and then lowered by an order of magnitude. For large diffusion, a rapid conduction of heat downward combined with the boundary condition of zero heat flux at the bottom would produce a tendency toward isothermality. With very small diffusion, stronger thermal stratification was expected. In essence small or weak diffusion caused temperature changes to be affected only by the convective and wind mixing processes. This is readily seen in Fig. 4a by the near horizontal sections of the $20^{o}C$ and $21^{o}C$ isotherms. The obvious

differences of Figs, 4a and 4b pointed out the importance of choosing a diffusion coefficient that did not overpower the other processes while simultaneously providing representative diffusion at depths to which the other processes did not extend. In order to accomplish these properties the value of 1.5 $cm^2 sec^{-1}$ was retained.

The next TYPE I experiment was designed to test the effects of the mixing parameterization. Computer runs were started with the same initial conditions except that the mixing parameterization was omitted. Figures 5a and 5b represent the basic TYPE I model without wind mixing. The striking similarity between Figs. 3a and 3b and Figs. 5a and 5b is readily apparent. Convection and diffusion alone performed the bulk of the heat transfer in the basic model. Wind mixing did not change the temperature profile extensively. It was therefore concluded that the basic asymmetry between spring and fall seen in the previous figures is due to the convective adjustment process and not due to mixing. Close inspection revealed that the important differences due to mixing occurred in autumn which was expected. In autumn the ocean was thermally stratified and most vulnerable to large downward eddy fluxes due to mixing. Of course the thermal stratification was greatest during summer but the wind was weak, causing a very shallow mixed-layer depth. In the case with no mixing, only diffusion and convection served to redistribute heat below the surface. Hence in summer when no convection was occurring in the top most layers, the

isotherms all tended to deepen at the same rate until autumn when convection finally had cooled the ocean down to that level. From this point on, convection dominated the vertical transport of heat. In the autumn, the deeper isotherms were pushed downward further with wind mixing occurring (Fig. 3a), than without mixing (Fig. 5a). This was because in the fall when the mixed layer was deepening, the requirement that the heat flux at -h be downward necessitated that the layer beneath -h be heated. In the winter, when the net surface flux was upward, the assumption that the flux at -h be downward (or zero) required that all levels above -h to cool at nearly the same rate, maintaining the stratification. The net result was a delay of the abrupt isothermal condition seen in Fig. 5a plus a continued deepening of low-level isotherms due to strong mixing.

Use of the Monin-Obukov length as a justifiable mixed-layer depth presupposed a stable fluid. During unstable conditions, this length was too small, however it was thought that convective adjustment would dominate the redistribution of heat in the layer. A comparison of a run in which mixing was allowed only in the stable case, (Fig. 6a) and mixing regardless of stability (Fig. 3a) was made. The definition of stability was made directly from the sign of the net surface flux. One can observe (Fig. 6a) a seeming discontinuity in autumn when mixing was abruptly cut off. Although the justification for using the Monin-Obukov length did not extend to unstable cases, the ocean temperature was still

stably stratified. In addition, with the stronger winds associated with winter, one expected mixing to at least the depth defined by the Monin-Obukov length. When stratified conditions are eroded, convective activity was expected to dominate and performed thusly. Therefore the decision was made to perform wind mixing throughout the year regardless of stability. Figure 3a was thus accepted as the TYPE I standard against which comparisons were made.

An additional comparison was made with the model employing a mixed-layer depth derived from mixed-layer theory. From Denman (1973), when mixing does not extend to the depth of the mixed layer, the mixed layer depth is determined by the following diagnostic equation;

$$h = \frac{G - D + \int_{-h}^{0} S(z)dz}{\frac{1}{2}\left[S_o + S_{-h} - (\overline{w'T'})_o\right]} \qquad (24)$$

Since the numerator was always positive as a consequence of the assumption of zero dissipation, one could see the sign of h was determined by the denominator. For this purpose, if one neglected S_{-h}, the remaining terms were proportional to surface flux. Since h was required to be positive, the corresponding surface flux was required to be downward or positive. Thus mixing was applicable only in the stable case. Figure 7 represents the mixing employing h derived from Eq. (24). It was found that this depth was always shallower than that from Monin-Obukov. The results compare with Fig. 6a. When a numerical comparison was made, the results showed that

the h from Eq. (24) varied from 30% to 80% of h_{mo}. However, for an h > 50 meters, the depth from Eq. (24) was at least 65% of h_{mo}. Since mixing was performed only when surface heat flux was downward, (or in April through September), one would expect h to be small due to lack of surface winds, which were at a minimum during that period.

From Eq. (15) one can see that there were virtually no restrictions on the magnitude of h. In fact, if Q approached zero, h would approach infinity. Therefore a restriction on the maximum value of h had to be devised. For finite differencing purposes, h had to be above the top of the lowest layer. A better physical maximum was that $h < w_*/f$. Various runs were made using each of the two restrictions. Since no problems were evident in either case, the better physical restriction that $h < w_*/f$ was retained.

B. TYPE II BOUNDARY CONDITIONS

As stated before, the TYPE II boundary condition specified the air temperature as a function of the time of the year. The predicted sea surface temperature from the model was then used with the specified air temperature in determining surface heat fluxes. Sensible and latent heat were specified

$$Q_H + Q_E = Q_2 (T_o - T_a(t))$$

where Q_2 was 70 ly day^{-1} $^oK^{-1}$ (Haney, 1971). The air temperature, $T_a(t)$, was specified as a cosine function plus a constant such that the net surface heat flux over the

annual cycle was close to zero. Longwave back radiation Q_B was set equal to a constant and Q_I was specified as a cosine function. Initial conditions of the model, similar to those of TYPE I, were isothermal. Also similar to TYPE I runs, each run was integrated through 20 years of time when an equilibrium was attained. It was thought that if the air temperature was significantly warmer or cooler than the ocean initially, then gradually the ocean would adjust and eventually reach an equilibrium state. The initial isothermal conditions was designed to minimize the transient stage.

TYPE II experiments were of two general categories; those dealing with the extrapolation which defines the ocean surface temperature and those dealing with comparisons against observations and TYPE I runs. The TYPE II conditions were purposely run in order to approximate more closely the conditions used in the three-dimensional baroclinic model (see section IIB) so the results would reflect the results of the large model when mixing scheme was introduced.

The model predicted the temperature at all ten levels, with the 10 meter temperature being the shallowest. This predicted temperature T_1 represents the average temperature when integrated over the depth of the top layer, 20 meters. Thus the actual surface temperature could be somewhat warmer than T_1. The temperature at 30_m was the predicted value T_2. If an isothermal layer was assumed to exist to an arbitrary depth $h' > 0$ (see Fig. 8) one could derive the following expression for the surface temperature;

$$T_{sfc} = T_1 \frac{(60 + h')}{2} - T_2 \left(\frac{20 - h'}{2}\right) \frac{1}{(h' + 20)} \qquad (25)$$

where the temperature at 20 meters was

$$T_{20m} = \frac{T_1 + T_2}{2}$$

It can be seen that if h'=0, such that no isothermal layer existed, then

$$T_{sfc} = 3/2\ T_1 - 1/2\ T_2 \qquad (26a)$$

and similarly

$$T_{sfc} = 7/6\ T_1 - 1/6\ T_2 \qquad \text{for } h'=10m \qquad (26b)$$

and

$$T_{sfc} = T_1 \qquad \text{for } h'=20m. \qquad (26c)$$

Figures 9, 10, and 11 were the results from the experiments corresponding to the extrapolations defined in Eqs. (26a, 26b, and 26c) respectively. No extrapolation exhibited undue sensitivity even though Fig. 11 displayed a secondary sea-surface temperature maximum in the fall. In fact each of the above extrapolations displayed this secondary maximum but it was not evident in all of the figures due to the contouring routine which drew only integer isotherms. The magnitude from relative minima to relative maximum in the secondary oscillation was $0.3^{o}K$. It appears that the extrapolations did cause the equilibrium heat content over the annual cycle to differ. In Eq. (25), the surface

temperature decreases with increasing h'. Thus for the coldest surface temperature, $T_{sfc}=T_1$, the ocean exhibited its largest heat content over the annual cycle. Remembering that air temperature was specified, the warmest surface extrapolation would equilibrate with cooler temperatures at levels one and two than the other extrapolations. Thus, the total heat content over the annual cycle seemed to be the only real difference of the three extrapolations. The value of T_{sfc} in Eq. (26b) was used in the three-dimensional baroclinic model.

Figure 12 shows the case with no mixing using TYPE II conditions. The result should be compared with Fig. 11 since h'=20 meters. The effects of mixing in the TYPE II model were significant. Not only did the mixing produce the same effects here as in TYPE I models, but it produced the secondary maximum. This occurred because in the early fall, mixing transported the heat down faster than it was coming in at the surface. This caused a short period in early September in which the flux at the bottom of the level exceeded the surface flux, causing a temporary cooling near the end of the warming season. This produced the local minimum followed by the secondary maximum in the early fall. The secondary maximum occurred because the downward flux into the upper level was greater than the downward flux to the second level. The downward flux out of the top level apparently decreased due to the increasing h. Comparisons between Figs. 11 and 12 readily show the gradual deepening of the isotherms

during summer due to diffusion. However, the local sea-surface temperature minimum in fall is not present in Fig. 12 nor is the delay of isothermal conditions. The conclusion was that both these effects were due to the mixing parameterization.

The TYPE I conditions (compare Fig. 3a and Fig. 11) displayed all the effects due to mixing stated above except for the local minimum in fall. The TYPE II boundary condition portrayed a much more complex interaction between ocean and atmosphere, whereas the TYPE I ocean was one that simply reacted to the atmosphere. One might expect that a stratified ocean subject to vigorous mixing due to autumn storms would cool the upper layers of the ocean through the downward transport of heat inherent in wind mixing. If the downward surface heat flux continued, warming the top layer, it would be reasonable to expect the local minimum. This premise presupposes strong mixing at a time when air temperature was not cooling at a fast rate. The phase relationship between mixing (seen in the magnitude of h) and surface flux would be critical to the presence of the secondary maximum.

The secondary maximum was not a phenomena found solely in the models shown here. Dorman et. al. (1974) found observations at Ocean Station "N" to have a late summer local minimum and a secondary maximum (Fig. 12). Although the time of occurence was not exactly the same in the model and in the observation, it must be remembered that the representation of air temperature (cosine function) specified in the model

had no phase angle nor did the wind from which h was calculated. Neither the initial conditions nor the boundary conditions were designed to represent Ocean Station "N," but the trends in the isotherms were expected to be similar. As stated before, the lack of steady state vertical motions caused the failure of a permanent thermocline to develop. In Fig. 13 , isotherms of 17°C and below could be considered part of the permanent thermocline.

Although in some ways Fig. 10 and Fig. 3 should resemble the observations in Fig. 13 in no way were they designed to represent that particular ocean station under the same conditions. The one-dimensional models shown here were for testing only. They were simplified grossly so that the complexities of the results from the three dimensional model could be more readily understood.

IV. THREE-DIMENSIONAL BAROCLINIC MODEL RESULTS

The three-dimensional baroclinic model began from rest with temperature a function of depth and latitude only. The model was integrated forward in time 5 years with constant forcing; that is using only the annual mean values of atmospheric parameters discussed in section IIb. This was done in an effort to reduce the initialization shocks and to "spin up" the currents to a quasi-steady state. Time dependency was introduced to the atmospheric parameters on the sixth year of integration and was continued for the rest of the integration. The mixing parameterization was introduced on the ninth year of integration, and the results shown below are for the tenth year.

The data of two points of geographical interest were saved every 5 days for later analyses. These were near Ocean Station November (30°N, 140°W) and Ocean Station Papa (50°N, 145°W). Both of these stations have been the subject of bathythermograph data collection since the late 1940's. As stated before, Fig. 13 represents the average data collected at Ocean Station November over a seven-year interval. The baroclinic model in its tenth year of integration produced Fig. 14 which shows the annual fluctuation of temperature from soundings taken every 5 days. The figure shows several aspects encountered in one dimensional test runs. The basic asymmetry of the isotherms is present as well as the

characteristic deepening of isotherms in summer months due to diffusion. However in fall the temperature pattern is typical of that seen in the no mixing case, Fig. 12a. The absence of a secondary maximum of any magnitude reinforces the belief that the mixing process in this model was very weak or completely absent. The conclusion drawn here was that the climatological winds provided too shallow a Monin-Obukov depth to produce any noticeable effect.

The permanent thermocline in the model, when compared to Fig. 13 , is too diffuse and as a result, the temperatures at depth (150m to 280m) were therefore too high. One possibility is that the vertical diffusion coefficient was too large or the vertical velocity "w" was of insufficient magnitude to support a permanent thermocline with a realistic gradient. Another possibility is that this deficiency, which also exists in other general circulation models (Bryan, 1975), may be due to the absence of a vertical eddy heat transport by baroclinic meso-scale eddies which are known to populate the real oceans. Finally, the magnitude of the surface temperatures was about $3^{o}C$ too large. This may have been simply due to the temperature forcing which was the surface air temperature averaged over the entire latitudinal belt. Clearly this type of averaging would tend to warm those normally cool points and cool those normally warm points. More precise forcing (individual data at each grid point) was unfeasible due to insufficiently accurate data, and computer storage restrictions.

The maximum and minimum surface temperatures in the model's "N" point occurred about the first of September and the first of March respectively. The observations from Dorman could not be compared for the maximum point due to the presence of the double maxima. However the middle of September seemed plausible if the local minimum had been absent. The minimum temperature occurred in the first half of April. Thus, although the time duration of the heating cycle was approximately correct, the phase lag with respect to observations was somewhat small. These discrepancies were not considered serious.

Another point was sampled for its temperature cycle. Ocean Station Papa manned by Canadian vessels was selected for comparisons. Figure 15 was produced with data from the tenth year of integration at the model's point corresponding to Papa's location.

Although a time dependent plot similar to Dorman's was not available, monthly data was available from Scripps Institute of Oceanography in the NORPAX project. The absence of a permanent thermocline at this latitude is in accordance with observations but the model's temperatures were also too warm here. Figure 15 also shows a lack of effects due to mixing. Since a time dependent plot of observations was not available, phase lag and duration were impossible to compare accurately with available data.

The three dimensional model, unlike the one dimensional models discussed above, had horizontal advection as an active heat transport mechanism. The seasonal variation of temperature advection is likely to be important for NORPAX goals. It did not appear to have an important role (compare Fig. 14 and Fig. 10) but has not been analyzed in this paper. This analysis is left for further study.

V. CONCLUSIONS

Although the baroclinic model did not perform up to expectations, most causes were clear and correctable. With proper initialization, a parameterization of storms which would give higher winds, plus an analysis of the diffuse permanent thermocline, it was thought that the baroclinic model could be used as a tool to study the evolution of the temperature anomalies in the North Pacific.

It has been shown that the climatological winds produced a forcing that made deep convective overturning dominant over other heat transport mechanisms. Thus on a model using climatological atmospheric parameters, the mixing parameterization may well be ignored or omitted. The model discussed in this work was one that could be coupled with an atmospheric model in which actual data could be used, thus providing the mixing parameterization the needed winds to perform adequately.

It was thought that the mixing parameterization, through the results shown in Section IIIb, produced effects on the temperature profile characteristic of actual mixing. Thus the model fulfilled in a large degree the initial purpose of better describing the upper ocean dynamics by incorporating the effects of surface-generated wind and convective mixing.

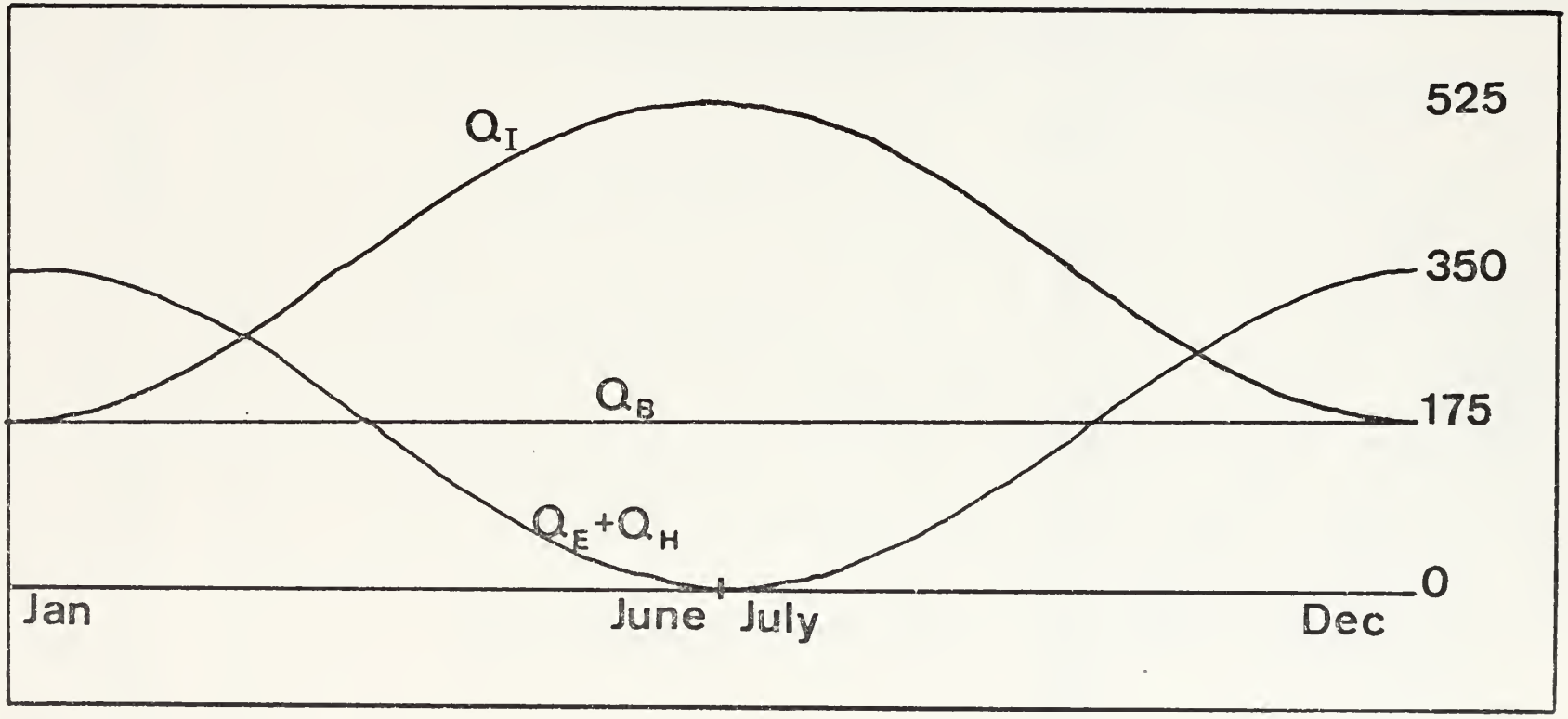

Figure 2. Representation of the surface flux boundary condition in the TYPE I model. Fluxes are in Langleys per day.

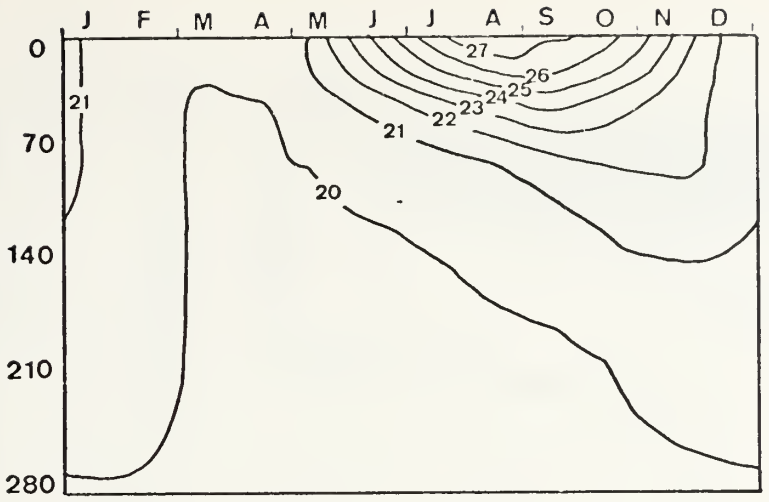

Figure 3a. The annual cycle of temperature distribution using TYPE I boundary conditions and mixing.

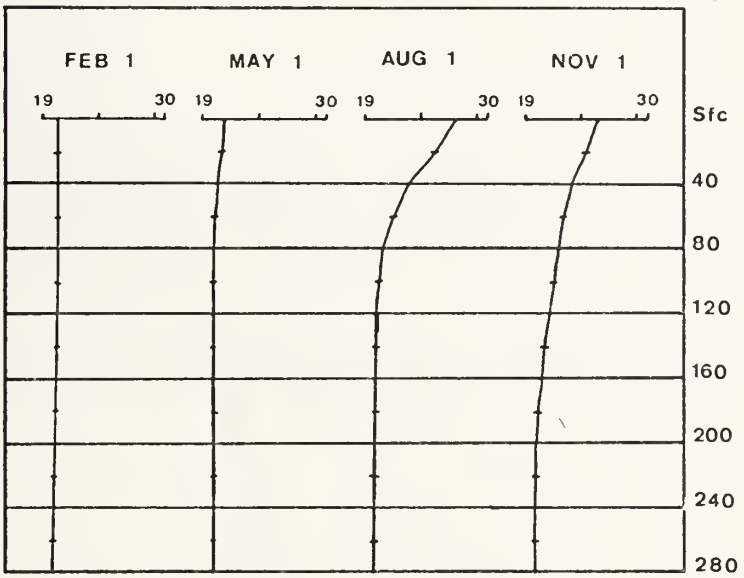

Figure 3b. Selected soundings from Fig. (3a).

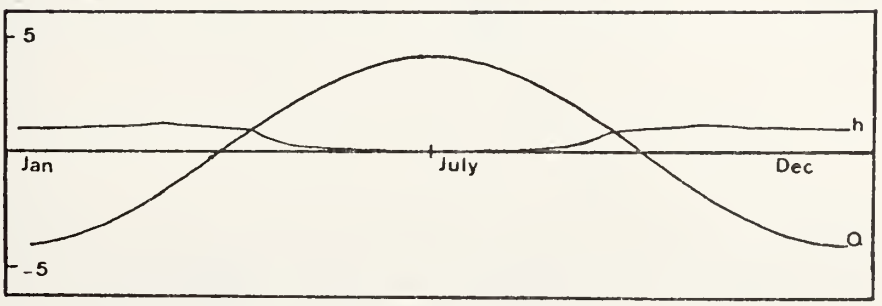

Figure 3c. Mixed layer depth h in hundreds of meters and surface heat flux Q in $cm^{o}k\ sec^{-1} \times 10^{-3}$.

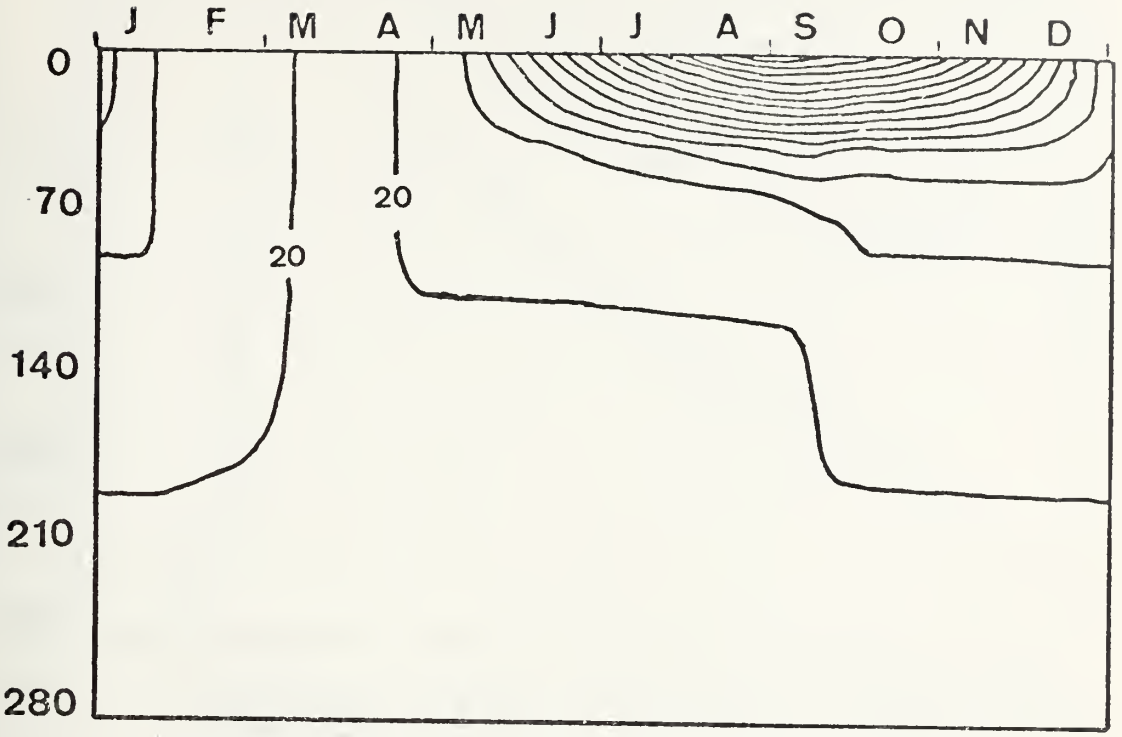

Figure 4a. The annual cycle of temperature distribution using TYPE I boundary condition with k=,15cm^{7}sec^{-1}.

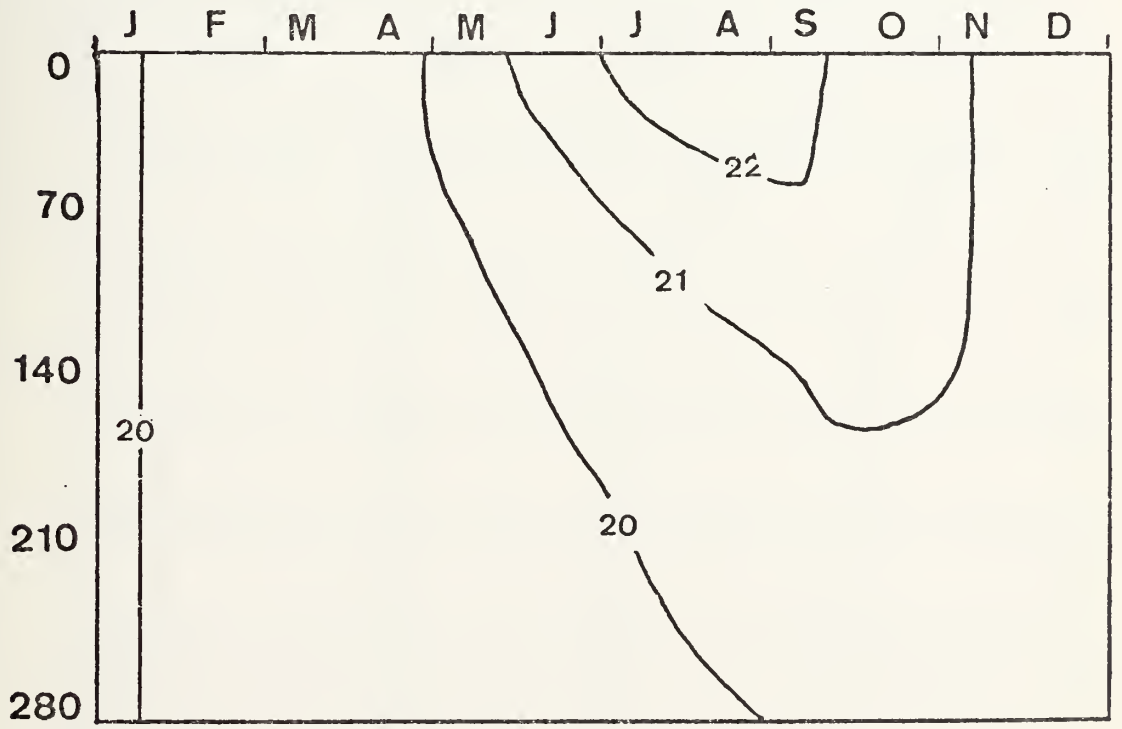

Figure 4b. The annual cycle of temperature distribution using TYPE I boundary conditions with k=15,0cm^{2}sec^{-1}.

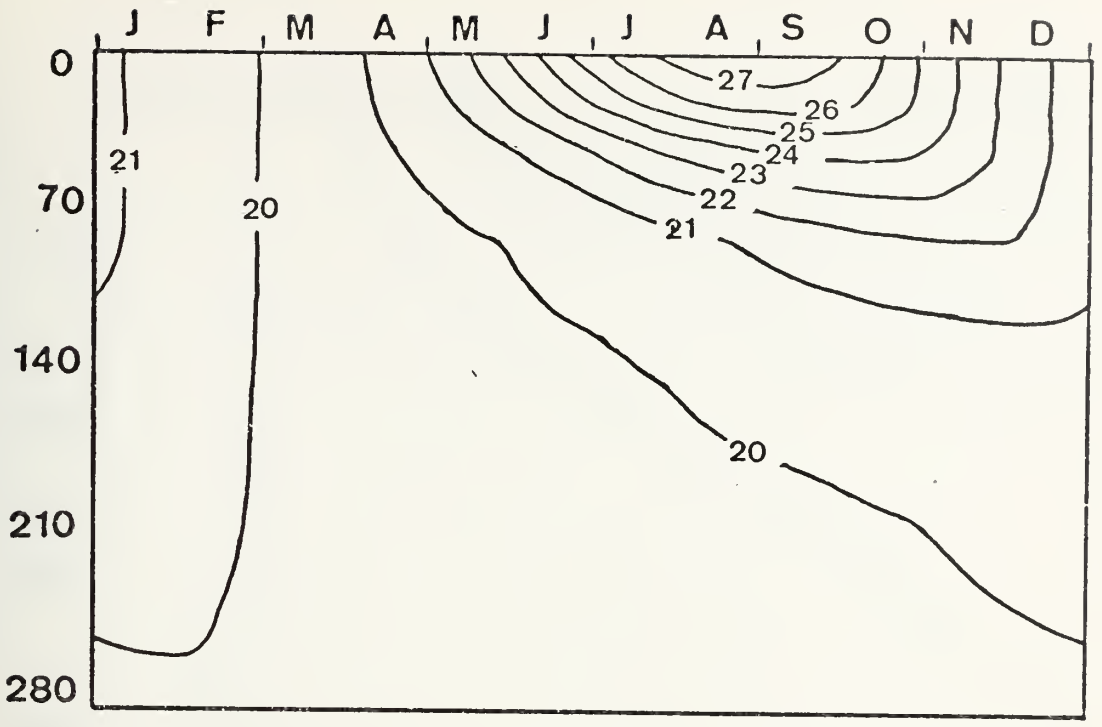

Figure 5a. The annual cycle of temperature distribution using TYPE I boundary condition with no mixing.

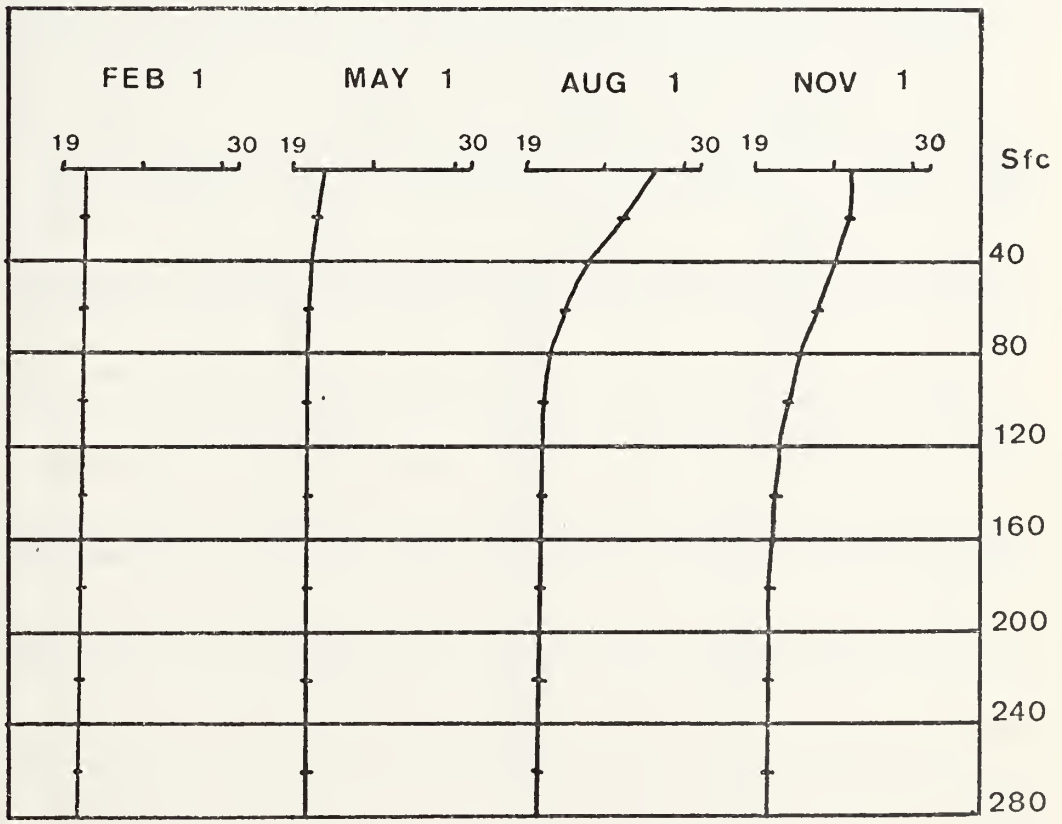

Figure 5b. Selected soundings from Fig. 5a.

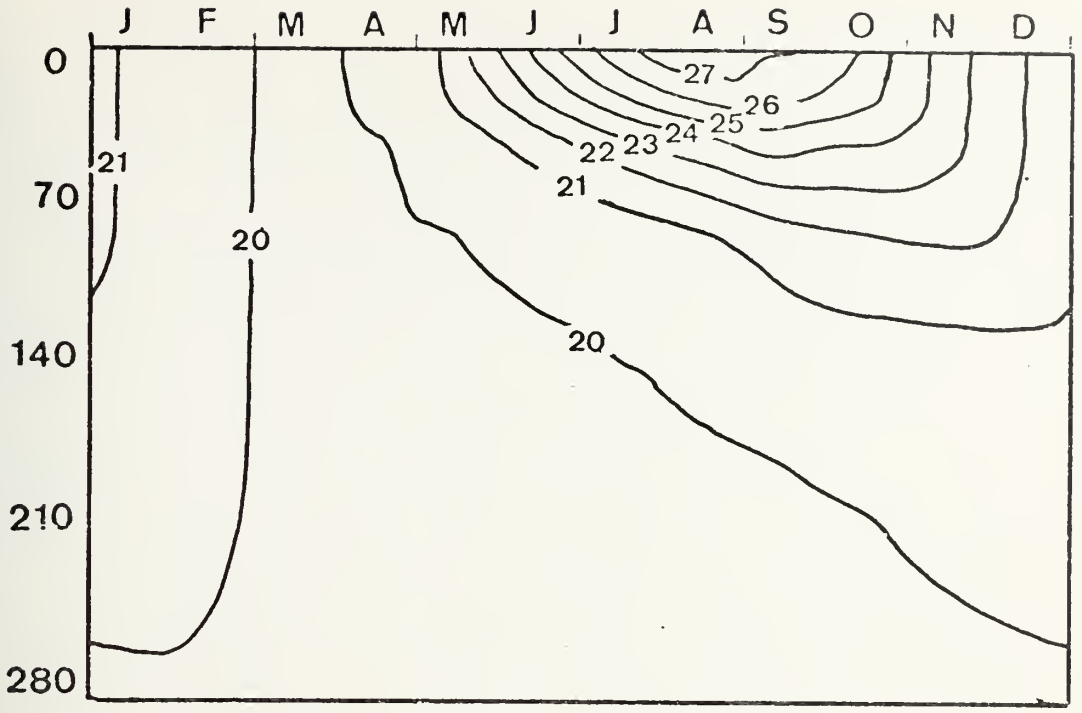

Figure 6a. The annual cycle of temperature distribution using TYPE I boundary conditions with mixing only in the Stable Case.

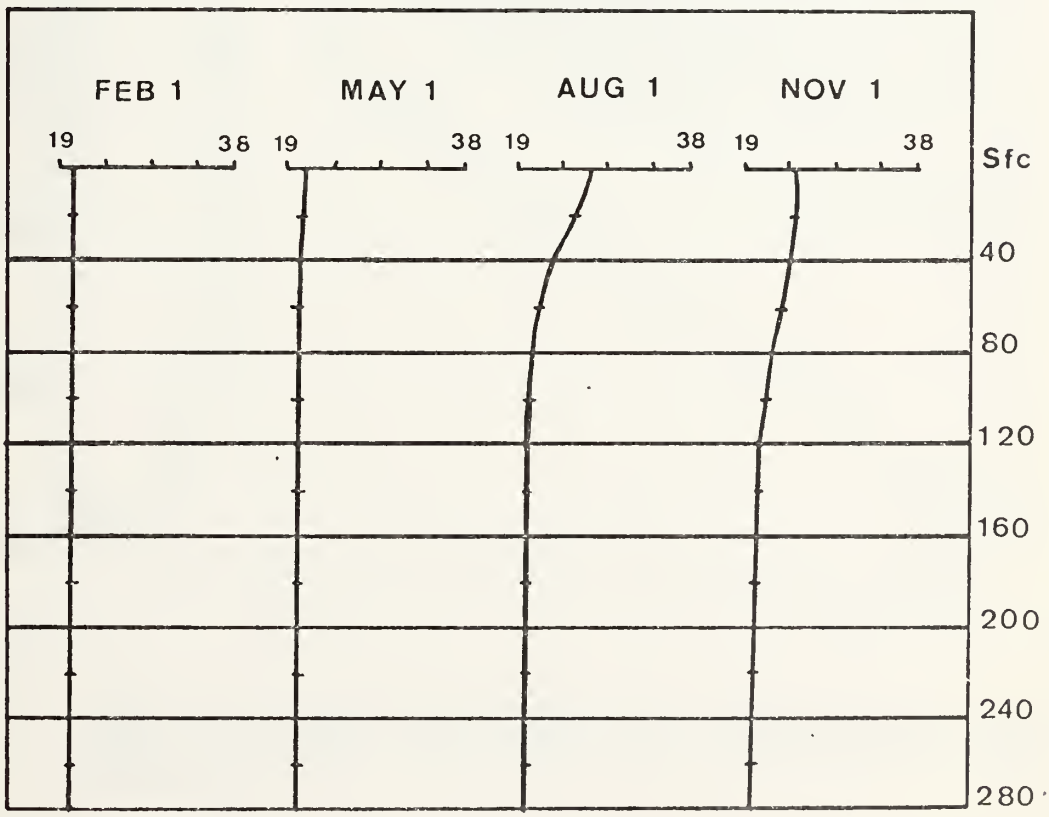

Figure 6a. Selected soundings from Fig. 6a.

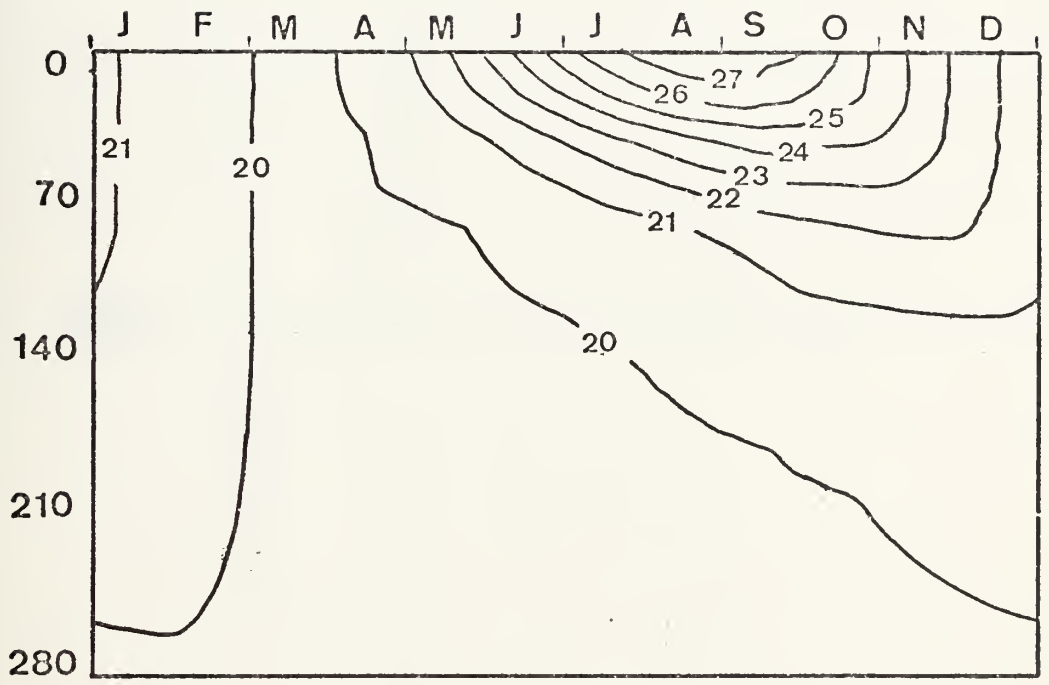

Figure 7. The annual cycle of temperature distribution using TYPE I boundary conditions with h calculated from Eq. (24).

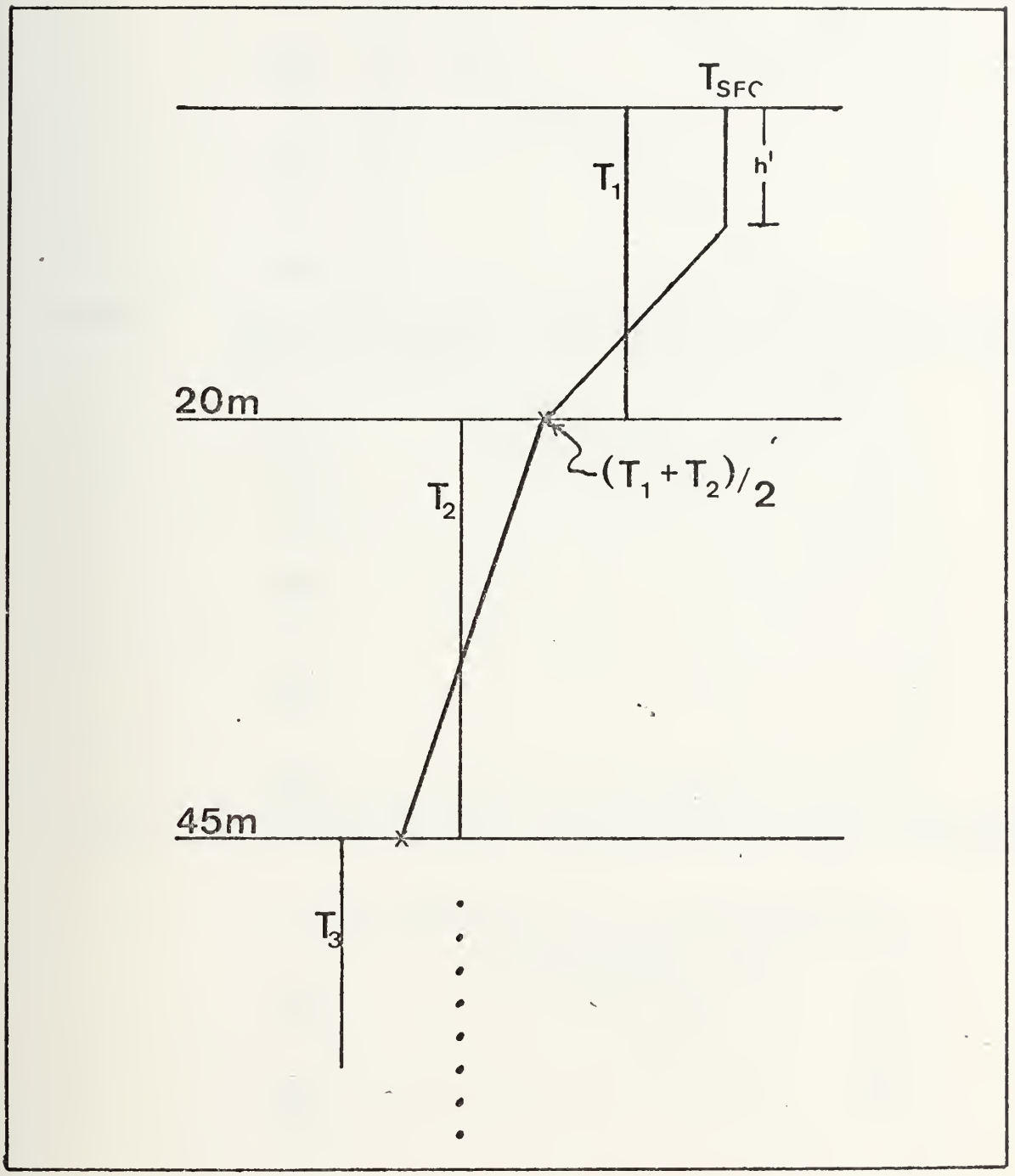

Figure 8. Representation of the extrapolation of sea surface temperature using an isothermal depth h'.

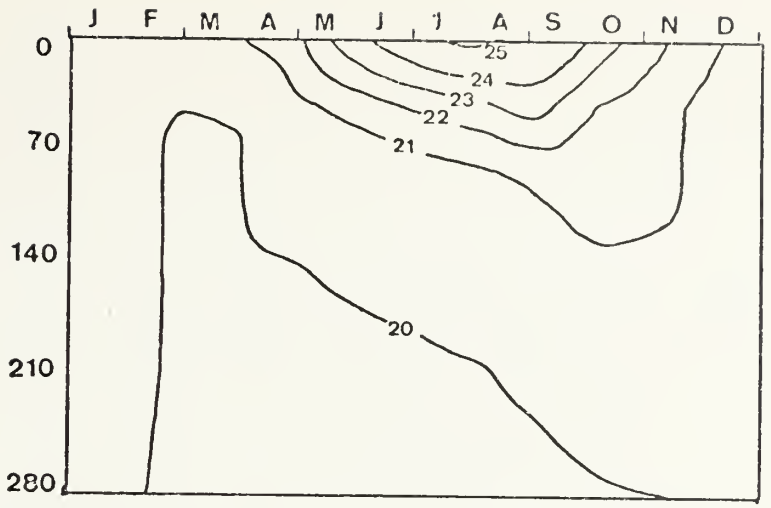

Figure 9. The annual cycle of temperature distribution using TYPE II boundary conditions with $T_{sfc}=3/2\ T_1-\frac{1}{2}T_2$.

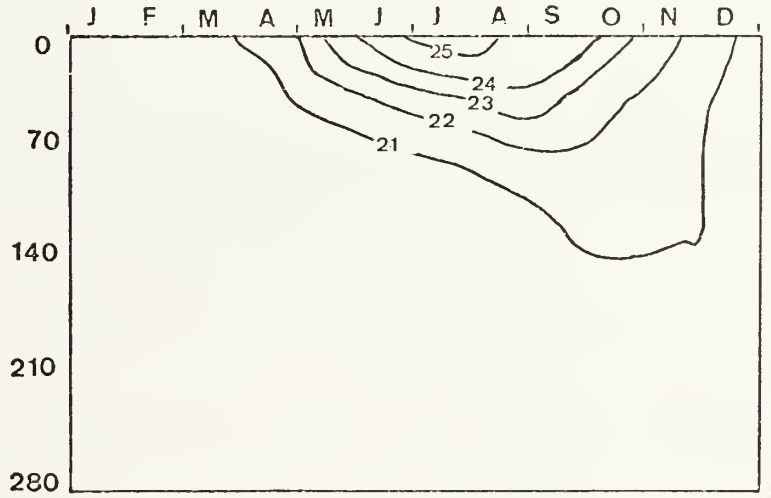

Figure 10. The annual cycle of temperature distribution using TYPE II boundary conditions with $T_{sfc}=7/6T_1-1/6T_2$.

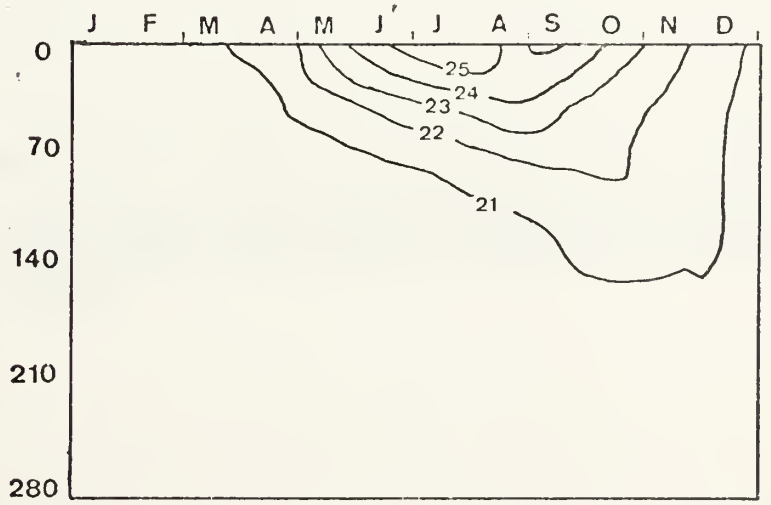

Figure 11. The annual cycle of temperature distribution using TYPE II boundary conditions with $T_{sfc}=T_1$.

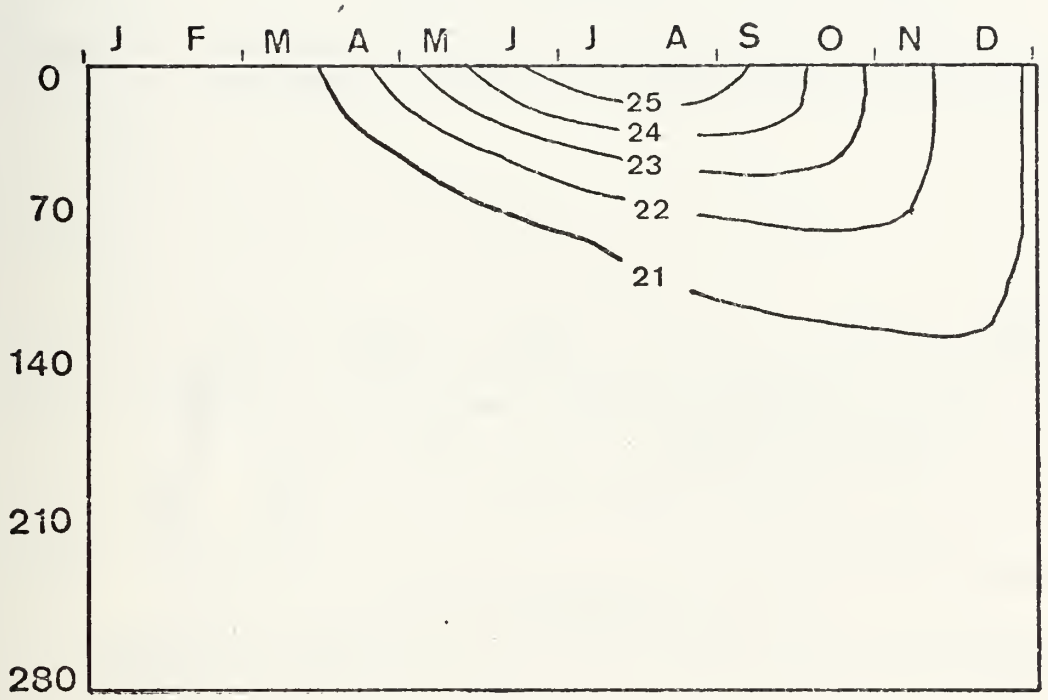

Figure 12. The annual cycle of temperature distribution using TYPE II boundary conditions with no mixing.

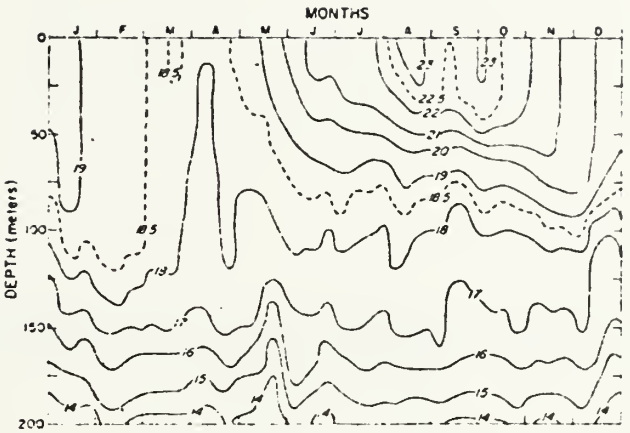

Figure 13. The annual cycle of temperature distribution at Ocean Station "N" from Dorman et al (1974).

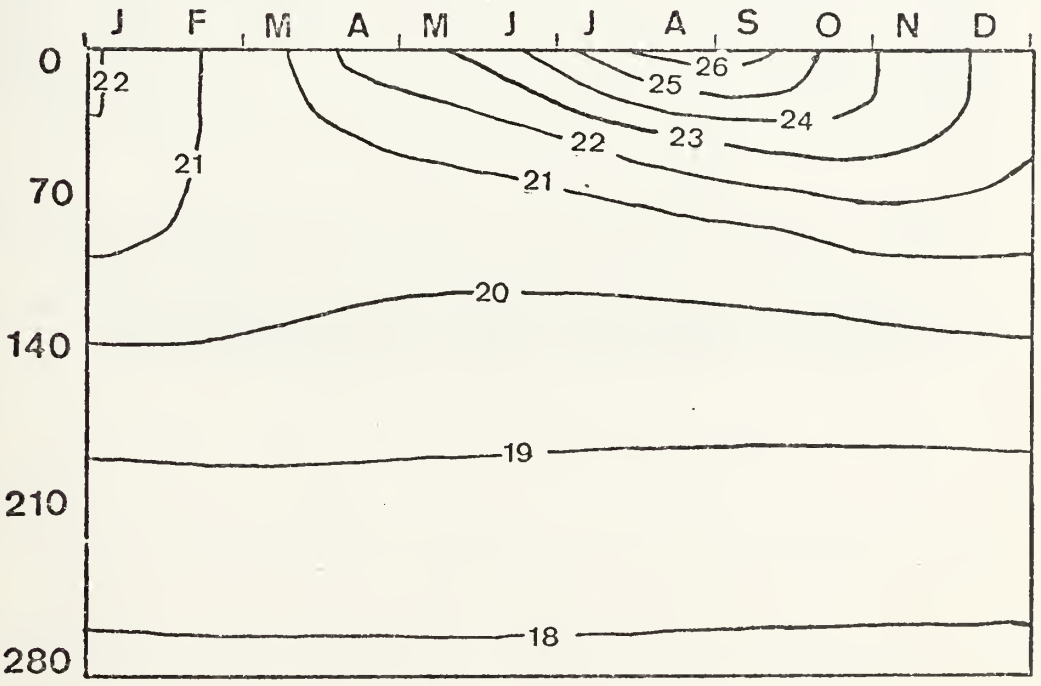

Figure 14. The annual cycle of temperature distribution predicted by the model from Ocean Station "N."

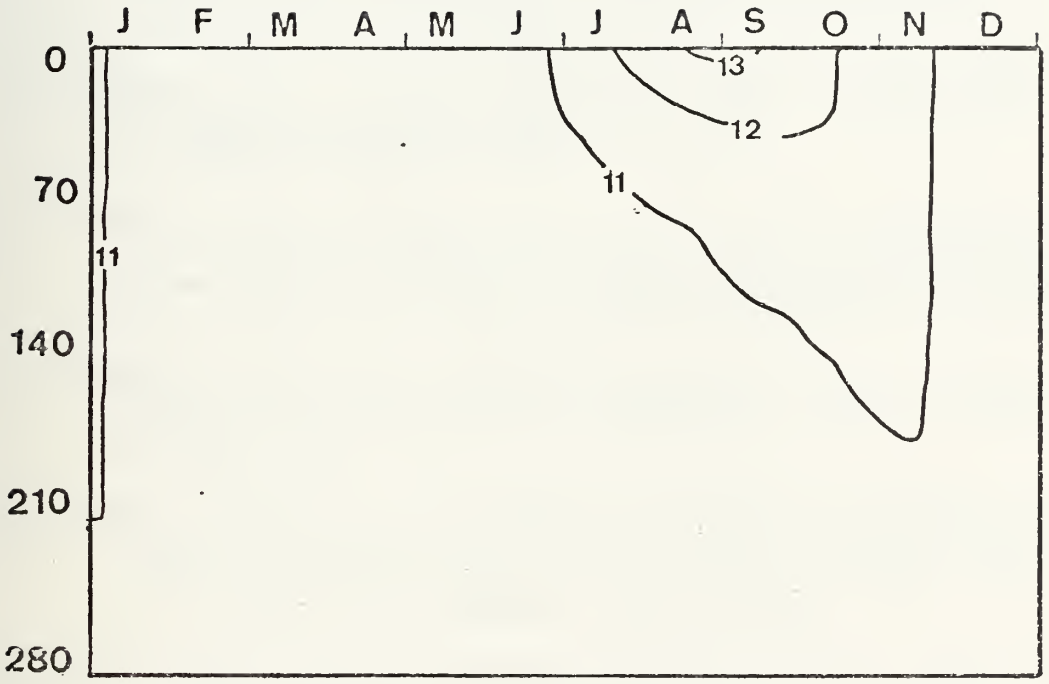

Figure 15. The annual cycle of temperature distribution predicted by the model for Ocean Station "P."

LIST OF REFERENCES

1. Born, R., Walker, A., Namias, J., White, W., "Monthly Mean Sea Surface Temperature Departures Over the North Pacific Ocean With Corresponding Subsurface Temperature Departures at Ocean Weather Stations "Victor," "Papa," and "November" from 1950 to 1970," SIO Ref. 73-28, 31 October 1973.

2. Bryan, K., Manabe, S., Pacanowski, R.C., "A Global Ocean Atmosphere Climate Model. Part II. The Ocean Circulation," Journal of Physical Oceanography, v. 5, no. 1, p. 30-46, January 1975.

3. Denman, K.L., "A Time Dependent Model of the Upper Ocean," Journal of Physical Oceanography, v. 3, no. 2, p. 173-184, April 1973.

4. Dorman, C.E., Paulson, C.A., Quinn, W.H., "An Analysis of 20 Years of Meteorological and Oceanographic Data from Ocean Station N," Journal of Physical Oceanography, v. 4, no. 4, p. 645-653, October 1974.

5. Hammond, Allen L., "Long-Range Weather Forecasting: Sea Temperature Anomalies," Science, v. 184, p. 1064-1065, 7 June 1974.

6. Haney, Robert L., "A Numerical Study of the Response of and Idealized Ocean to Large-Scale Surface Heat and Momintum Flux," Journal of Physical Oceanography, v. 4, no. 2, p. 145-167, April 1974.

7. Hellerman, S., "An Updated Estimate of the Wind Stress on the World Ocean," Monthly Weather Review, v. 96, p. 63-74, January 1968.

8. Jenne, R.L., Crutcher, H.L., van Loon, H., Talijaard, J.J., "Climate of the Upper Air; Part II Northern Hemisphere; Vol. III; Geostrophic Winds." 1974.

9. Kraus, E.B., Turner, J.S., "A One-Dimensional Model of the Seasonal Thermocline: II The General Theory and Its Consequences," Tellus, v. 19, p. 98-106, 1967.

10. List, R.J., Smithsonian Meteorological Tables, Smithsonian Institute, Washington, D.C., p. 527, 1963.

11. Miller, D.B., Feddes, R.G., Global Atlas of Relative Cloud Cover, p. 237, 1971.

12. Munk, Walter H., "Abyssal Recipes," Deep Sea Research, v. 13, p. 707-730, 1966.

13. Namias, J., "Seasonal Interactions Between the North Pacific Ocean and the Atmosphere During the 1960's," Monthly Wx Review, v. 97, no. 3, p. 173-192, March 1969.

14. Paulson, C.A., Simpson, J.J., "Absorption of Solar Radiation in the Upper Ocean," paper presented at Fall annual meeting of the A.G.U., San Francisco, California, 12 December 1974.

15. Phillips, O.M., The Dynamics of the Upper Ocean, Cambridge University Press, p. 222-235, 1966.

16. Sweet, Roland A., "A Direct Method for Solving Poisson's Equation," NCAR Report, no. 22, September 1972.

INITIAL DISTRIBUTION LIST

		No. Copies
1.	Defense Documentation Center Cameron Station Alexandria, Virginia 22314	2
2.	Library (Code 0212) Naval Postgraduate School Monterey, California 93940	2
3.	Prof. R. L. Haney Code 51Hy Department of Meteorology Naval Postgraduate School Monterey, California 93940	3
4.	R. W. Davies 2346 Carol Avenue Mountain View, California 94040	3
5.	Meteorology Department Code 51 Library Naval Postgraduate School Monterey, California 93940	1
6.	Oceanography Department Code 58 Library Naval Postgraduate School Monterey, California 93940	1
7.	Naval Oceanographic Office Library (Code 3330) Washington, D. C. 20373	1
8.	Commander Naval Weather Service Command Naval Weather Service Headquarters Washington Navy Yard Washington, D. C. 20390	1
9.	Fleet Numerical Weather Center Naval Postgraduate School Monterey, California 93940	1
10.	Prof. R. L. Elsberry Code 51Es Department of Meteorology Naval Postgraduate School Monterey, California 93940	1

11. Dr. W. L. Gates 1
Physical Science Department
1700 Main Street
Santa Monica, California 90406

12. B. Kagan 1
Institute of Oceanography
Academy of Sciences USSR
5, Universitetskaya Naberezhnaya
Leningrad W-164, USSR

13. R. O. R. Y. Thompson 1
Woods Hole Oceanographic Institution
Woods Hole, Massachusetts 02543

14. Professor G. J. Haltiner, Chairman 1
Department of Meteorology
Naval Postgraduate School
Monterey, California 93940

Thesis 160610
D1692 Davies
c.1 A numerical parameterization of wind mixing in a time dependent baroclinic oceanic general circulation model.